Task-Oriented Accuracy Measure for Dexterous Manipulation

Masahito Yashima and Tasuku Yamawaki
Dept. of Mechanical Systems Engineering
National Defense Academy of Japan
1-10-20 Hashirimizu, Yokosuka, Japan
{yashima & yamawaki}@nda.ac.jp

***Abstract*—The present paper proposes a novel quality measure for choosing a grasp with high task accuracy to achieve a specified task. In precision manipulation tasks such as a peg-in-hole insertion, the task accuracy required for each direction in the task space is different. It is required to choose the grasp which meets with specified task requirements. According to the linear system theory, the task-oriented accuracy measure is derived by using the singular values of the output controllability matrix for the manipulation system. The usefulness of the proposed quality measure are shown by two simulations concerning a peg-in-hole insertion task and a baton twirling.**

***Index Terms*—grasp quality measure, task-oriented measure, dexterous manipulation, robotic hand**

I. INTRODUCTION

The present paper proposes a novel quality measure for choosing a grasp with high task accuracy to achieve a specified task. There can be an infinite number of possible grasps for a particular task because there are many choices of the hand configurations, contact locations and contact forces. In order to choose the high quality grasp for dexterous manipulation, several measures to evaluate a grasp have been proposed [1], [3], [7], [9], [10], [13].

The grasp stability measure has been developed by using the concept of a wrench space to evaluate the ability to resist statically external forces and torques which are exerted on the object without the object slipping from the grasp. The set of all the possible wrenches that can be applied to the object is called the grasp wrench space. In [3], [7], the radius of the largest wrench ball which fits within the grasp wrench space was proposed as a quality measure.

However, since these grasp stability measures are not related to the task to be performed, the use of these measures do not always result finding the optimal grasp for the specified task. The choice of a grasp for dexterous manipulation should be based on its capability to realize the specified task [9].

In order for a robotic hand to be used in a wider range of operations, the robotic hand is required not only to grasp the object firmly against the external forces but to manipulate the object accurately. Several manipulation tasks such as a peg-in-hole insertion and a manipulation with tweezers are taken as typical examples of the precision manipulation, as shown in Fig. 1, According as a specified task, the task accuracy required for each direction in the task space is different. In order to choose the grasp which meets with each specified task accuracy requirement, a task accuracy measure, which is different from the conventional stability measure, is required. To our knowledge, there has been few study on the task accuracy measure to evaluate a grasp.

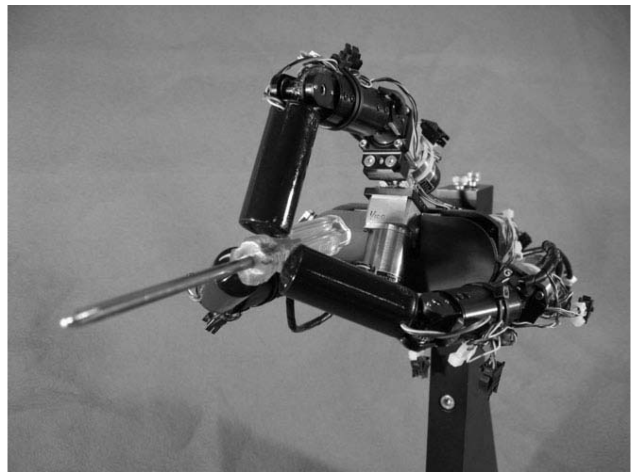

Fig. 1. The NDA Hand executing an accurate manipulation task

According to the linear system theory, the magnitudes of the singular values and the corresponding singular vectors of the output controllability matrix for a control system represent the intensity of the effect of inputs on outputs and the corresponding directions, respectively [4], [5]. The idea has been applied to the sensitivity analysis of the control system.

If we regard the manipulation system as a system whose inputs and outputs are the joint torques of the fingers and the object's position and orientation, respectively, the above-mentioned concept can be applied to the grasp evaluation on the basis of a take accuracy. We have revealed that the idea is effective in the motion planning of a manipulator so as to reduce the magnitude of the positional error at the goal point of the trajectory [15], [16].

In the present paper, we propose the task accuracy measure for a given task by using the concept of output controllability. Section II derives the linearized model of a manipulation system. In section III, the task-oriented accuracy measure is derived by using the singular values of the output controllability matrix. As application examples using the proposed quality measure, section IV shows two simulation results concerning a peg-in-hole insertion task and a baton twirling.

II. Linearized Model

A. Kinematic Constraints

A manipulation system consists of an object and a multi-fingered hand in the three dimensional space. It is assumed that the multi-fingered hand is non-redundant, or the hand has three fingers and each finger has three joints [12]. As an example of a hand like this, Fig. 2 shows the NDA Hand, which was developed in our laboratory [17].

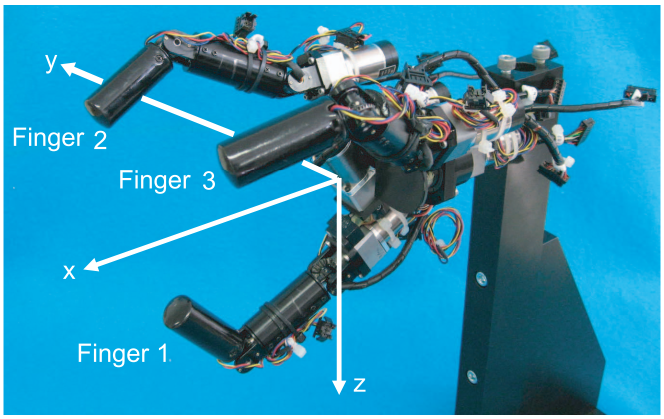

Fig. 2. The NDA Hand which consists of three three-jointed fingers

Let $\boldsymbol{x}_O = \left[\begin{array}{cc} \boldsymbol{p}_O^T & \boldsymbol{\phi}_O^T \end{array}\right]^T \in \Re^6$ denote the position $\boldsymbol{p}_O$ and orientation $\boldsymbol{\phi}_O$ of the object, whose frame is fixed to the object mass center. Let $\boldsymbol{\theta} \in \Re^{3n_f}$ be the vector of the joint angle of the n_f-fingers. Assuming that the distal link of each finger makes a frictional point contact with the object and that sliding does not occur at any contact points by applying appropriate contact forces, the velocity constraints between $\dot{\boldsymbol{x}}_O$ and $\dot{\boldsymbol{\theta}}$ can be described as [12]

$$\boldsymbol{W}_O^T \, \dot{\boldsymbol{x}}_O = \boldsymbol{J}\dot{\boldsymbol{\theta}} \tag{1}$$

where $\boldsymbol{J} \in \Re^{3n_f \times 3n_f}$ is the hand Jacobian. Since each finger has three degrees of freedom as mentioned above, the Jacobian $\boldsymbol{J}$ becomes square matrix and the multi-fingered hand results in non-redundant. The matrix $\boldsymbol{W}_O^T \in \Re^{3n_f \times 6}$ is the grasp matrix, which relates $\dot{\boldsymbol{x}}_O$ with the velocity vector at the contact points.

B. Dynamics of Manipulation System

The equation of motion for the multi-fingered hand are given by

$$\boldsymbol{M}_H\ddot{\boldsymbol{\theta}} + \boldsymbol{h}_H + \boldsymbol{g}_H = \boldsymbol{\tau} - \boldsymbol{J}^T\boldsymbol{f}_C \tag{2}$$

where $\boldsymbol{M}_H \in \Re^{3n_f \times 3n_f}$ is the inertia matrix, $\boldsymbol{h}_H \in \Re^{3n_f}$, $\boldsymbol{g}_H \in \Re^{3n_f}$, $\boldsymbol{\tau} \in \Re^{3n_f}$ and $\boldsymbol{f}_C \in \Re^{3n_f}$ are the vectors of the Coriolis term, the gravitational term, joint torques, and components of the contact forces exerted by the fingers at their contact points, respectively.

The equation of motion for the object are described as

$$\boldsymbol{M}_O\ddot{\boldsymbol{x}}_O + \boldsymbol{h}_O + \boldsymbol{g}_O = \boldsymbol{W}\boldsymbol{f}_C \tag{3}$$

where $\boldsymbol{M}_O \in \Re^{6\times 6}$ is the inertia matrix of the object, and $\boldsymbol{h}_O \in \Re^6$ and $\boldsymbol{g}_O \in \Re^6$ are the vectors of the Coriolis and gravitational terms, respectively.

The contact forces generating the acceleration of the object can be derived from (3), which are [12]

$$\boldsymbol{f}_C = \boldsymbol{W}^\sharp(\boldsymbol{M}_O\ddot{\boldsymbol{x}}_O + \boldsymbol{h}_O + \boldsymbol{g}_O) + \boldsymbol{f}_I \tag{4}$$

where $\boldsymbol{W}^\sharp$ is the pseudo inverse of the wrench matrix $\boldsymbol{W}$. The first term of (4) represents manipulating force which produces the resultant force and moment exerted on the object. The second term represents an internal force $\boldsymbol{f}_I$, which should be determined so that the contact force $\boldsymbol{f}_C$ could satisfy the friction constraint without the fingers slipping on the object.

The acceleration constraints are obtained by differentiating the velocity constraint (1). When the matrix $\boldsymbol{J}$ is invertible, the joint angular acceleration $\ddot{\boldsymbol{\theta}}$ can be given by

$$\ddot{\boldsymbol{\theta}} = \boldsymbol{J}^{-1}(\boldsymbol{W}_O^T\ddot{\boldsymbol{x}}_O + \dot{\boldsymbol{W}}_O^T\dot{\boldsymbol{x}}_O - \dot{\boldsymbol{J}}\dot{\boldsymbol{\theta}}) \tag{5}$$

Substituting (4) and (5) into (2) yields the dynamic equations for the whole manipulation system, which are

$$\boldsymbol{M}_{\text{sys}}\left[\begin{array}{c} \ddot{\boldsymbol{x}}_O \\ \boldsymbol{f}_I \end{array}\right] = \boldsymbol{\tau} - \boldsymbol{h}_{\text{sys}} - \boldsymbol{g}_{\text{sys}} \tag{6}$$

where $\boldsymbol{M}_{\text{sys}}$, $\boldsymbol{h}_{\text{sys}}$ and $\boldsymbol{g}_{\text{sys}}$ indicate the inertia matrix, and the vectors of the Coriolis term and the gravitational term for the whole manipulation system, respectively.

Since the hand is assumed to be non-redundant, $\boldsymbol{M}_{\text{sys}} \in \Re^{3n_f\times 3n_f}$ in (6) becomes a square matrix. When $\boldsymbol{M}_{\text{sys}}$ is invertible, solving for $[\ddot{\boldsymbol{x}}_O^T \; \boldsymbol{f}_I^T]^T$ on the left-hand side of (6) yields

$$\left[\begin{array}{c} \ddot{\boldsymbol{x}}_O \\ \boldsymbol{f}_I \end{array}\right] = \boldsymbol{M}_{\text{sys}}^{-1}(\boldsymbol{\tau} - \boldsymbol{h}_{\text{sys}} - \boldsymbol{g}_{\text{sys}}) \tag{7}$$

We devide the matrix $\boldsymbol{M}_{\text{sys}}^{-1}$ into the two matrices such as

$$\boldsymbol{M}_{\text{sys}}^{-1} = \left[\begin{array}{c} \boldsymbol{\Lambda}_O \\ \boldsymbol{\Lambda}_f \end{array}\right]$$

Thus, the acceleration of the object $\ddot{\boldsymbol{x}}_O$ and the internal force $\boldsymbol{f}_I$, which are generated by the applied joint torque $\boldsymbol{\tau}$, can be written as follows:

$$\ddot{\boldsymbol{x}}_O = \boldsymbol{\Lambda}_O(\boldsymbol{\tau} - \boldsymbol{h}_{\text{sys}} - \boldsymbol{g}_{\text{sys}}) \tag{8}$$

$$\boldsymbol{f}_I = \boldsymbol{\Lambda}_f(\boldsymbol{\tau} - \boldsymbol{h}_{\text{sys}} - \boldsymbol{g}_{\text{sys}}) \tag{9}$$

C. State Equation and Output Equation

We consider the dynamic property between the acceleration of the object $\ddot{\boldsymbol{x}}_O$ and the joint torque $\boldsymbol{\tau}$ in order to derive a task-oriented quality measure for dexterous manipulation. Since the model (8) is still intractable, we derive the linearized dynamic model of (8). It is assumed that the appropriate internal forces $\boldsymbol{f}_I$ in (9) are applied at contact points without the fingers slipping on the object.

Linearizing (8) with respect to the equilibrium points $\boldsymbol{x}_O = \boldsymbol{x}_{Oe}$, $\boldsymbol{\theta} = \boldsymbol{\theta}_e$, $\boldsymbol{\xi} = \boldsymbol{\xi}_e$, $\boldsymbol{\tau} = \boldsymbol{\tau}_e$ and $\boldsymbol{p} = \boldsymbol{p}_e$, which satisfy $\ddot{\boldsymbol{x}}_O = \dot{\boldsymbol{x}}_O = \boldsymbol{0}$, $\ddot{\boldsymbol{\theta}} = \dot{\boldsymbol{\theta}} = \boldsymbol{0}$, and $\ddot{\boldsymbol{\xi}} = \dot{\boldsymbol{\xi}} = \boldsymbol{0}$, yields the linear time-invariant state equation and output equation as follows:

$$\delta\dot{\boldsymbol{z}} = \boldsymbol{A}\delta\boldsymbol{z} + \boldsymbol{B}\delta\boldsymbol{\tau} \tag{10}$$

$$\delta\boldsymbol{p} = \boldsymbol{C}\delta\boldsymbol{z} \tag{11}$$

where $\delta\boldsymbol{z} = \begin{bmatrix} \delta\boldsymbol{x}_O^T & \delta\dot{\boldsymbol{x}}_O^T \end{bmatrix}^T$ is state variables, $\delta\boldsymbol{\tau} = \boldsymbol{\tau} - \boldsymbol{\tau}_e$ is input variables and $\delta\boldsymbol{p} = \boldsymbol{p} - \boldsymbol{p}_e$ is output variables. The $\boldsymbol{p} \in \Re^6$ is the vector of position and orientation at the specified point on the object. Coefficient matrices in (10) and (11) can be written by

$$\boldsymbol{A} = \begin{bmatrix} \boldsymbol{0} & \boldsymbol{I}_6 \\ -\boldsymbol{\Lambda}_O\boldsymbol{G} & \boldsymbol{0} \end{bmatrix}_{\substack{x_O = x_{Oe} \\ \theta=\theta_e \\ \xi=\xi_e}}, \quad \boldsymbol{B} = \begin{bmatrix} \boldsymbol{0} \\ \boldsymbol{\Lambda}_O \end{bmatrix}_{\substack{x_O = x_{Oe} \\ \theta=\theta_e \\ \xi=\xi_e}} \\ \boldsymbol{C} = \begin{bmatrix} \boldsymbol{S} & \boldsymbol{0} \end{bmatrix} \tag{12}$$

where the matrix $\boldsymbol{I}_6$ is a 6×6 identity matrix, the matrix $\boldsymbol{0}$ is a zero matrix, $\boldsymbol{G} = \partial\boldsymbol{g}_{\text{sys}}/\partial\boldsymbol{x}_O$, and $\boldsymbol{S} \in \Re^{6\times 6}$ is the matrix which relates $\delta\boldsymbol{x}_O$ with the output variables $\delta\boldsymbol{p}$.

III. Task Accuracy Measure

A. Output Controllability

A system is said to be output controllable if it is possible to construct inputs that will transfer any given initial output to any final output until a finite time [6], [8]. When a manipulation system shown in (10) and (11) is output controllable, there exist joint torques $\delta\boldsymbol{\tau}$ which move the object to arbitrary position and orientation $\delta\boldsymbol{p}$ until a finite time. The output controllability matrix $\boldsymbol{N}$ of the manipulation system can be obtained using the matrices $\boldsymbol{A}$, $\boldsymbol{B}$ and $\boldsymbol{C}$ of (12), which is

$$\begin{aligned} \boldsymbol{N} &= \boldsymbol{C}\begin{bmatrix} \boldsymbol{B} & \boldsymbol{A}\boldsymbol{B}\cdots\boldsymbol{A}^{11}\boldsymbol{B} \end{bmatrix} \\ &= \Big[\, \boldsymbol{0} \quad \boldsymbol{\Lambda}_O \quad \boldsymbol{0} \quad (-\boldsymbol{\Lambda}_O\boldsymbol{G})\boldsymbol{\Lambda}_O \cdots \\ &\qquad \cdots(-\boldsymbol{\Lambda}_O\boldsymbol{G})^{11}\boldsymbol{\Lambda}_O \Big] \end{aligned} \tag{13}$$

The subspace of the output-controllable object's position and orientation $\delta\boldsymbol{p}$ steered by the input joint torque $\delta\boldsymbol{\tau}$ is equivalent to the range space of the output controllability matrix $\boldsymbol{N}$, which is [6]

$$\text{Range } \boldsymbol{N} = \{\delta\boldsymbol{p} \in \Re^6 \mid \delta\boldsymbol{p} = \boldsymbol{N}\delta\hat{\boldsymbol{\tau}}, \ ^{\forall}\delta\hat{\boldsymbol{\tau}}\} \tag{14}$$

where $\delta\hat{\boldsymbol{\tau}} = [\delta\hat{\boldsymbol{\tau}}_1^T, \ \delta\hat{\boldsymbol{\tau}}_2^T, \ldots, \ \delta\hat{\boldsymbol{\tau}}_{3n_f}^T]^T$, $\delta\hat{\boldsymbol{\tau}}_i = \int_0^{t_f} q_i(-t)\delta\boldsymbol{\tau}(t)dt$, $q_i(t)$ is some scalar function of time, and $t_f > 0$ is an arbitrary time.

According to the linear system theory [14], the characteristic of the output-controllable $\delta\boldsymbol{p}$ steered by the input joint torque $\delta\boldsymbol{\tau}$ can be found by the singular value decomposition of the output controllability matrix $\boldsymbol{N}$, which is

$$\boldsymbol{N} = \sum_{i=1}^{6} \sigma_{Ni}\boldsymbol{u}_{Ni}\boldsymbol{v}_{Ni}^T \tag{15}$$

where $\sigma_{N1} \geq \sigma_{N2} \geq \ldots \geq \sigma_{N6} > 0$ are the singular values, and $\boldsymbol{u}_{Ni}$ is a corresponding singular vector.

The magnitudes of the singular values represent the strengths of the effects of input on output [4], [5], [11]. When the object is steered in the direction of the maximum singular vector $\boldsymbol{u}_{N1}$, the effect of the joint driving force (input) on the object's position and orientation (output) is maximized. Therefore, the task accuracy is the lowest since even small external forces greatly affect the motion of the object in this direction.

In contrast, the effect of the joint driving torque (input) on the object's position and orientation (output) is the lowest in the direction of the minimum singular vector $\boldsymbol{u}_{N6}$. Therefore, the task accuracy is the highest in this direction in which the manipulation system has the lowest-sensitivity.

In the above discussion, we have assumed that there is no constraint imposed on the maximum joint driving torques $\boldsymbol{\tau}$ and that the weights of the components related to the translational and rotational motion of the object, $(\boldsymbol{p}_O, \ \boldsymbol{\phi}_O)$, are the same. When these assumptions do not hold, normalization of inputs and/or outputs variables is needed.

B. Task-oriented Measure

According as a specified task, the task accuracy required for each direction in the task space is different. For example, in the case of a peg-in-hole insertion, as shown in Fig. 3, high task accuracy is not always needed in the insertion direction, while the motion along with the rest of directions in the task space generally requires higher task accuracy in order to prevent the object from colliding with an environment.

In order to choose the grasp which meets specified task accuracy requirements, we consider a weighting output controllability matrix $\boldsymbol{N}_T$, which is derived from the product of the output controllability matrix $\boldsymbol{N}$ and a weighting matrix $\boldsymbol{T}$ as follows:

$$\boldsymbol{N}_T = \boldsymbol{T}\boldsymbol{N} \tag{16}$$

where

$$\boldsymbol{T} = \text{diag}(w_1, \ \cdots, w_6), \tag{17}$$

and the w_i indicates a weight for the required task accuracy of $\delta\boldsymbol{p}_i$, which is the ith element of the output variables $\delta\boldsymbol{p}$.

The higher task accuracy the object's motion in the direction of $\delta\boldsymbol{p}_i$ requires, the larger we make the value of weight

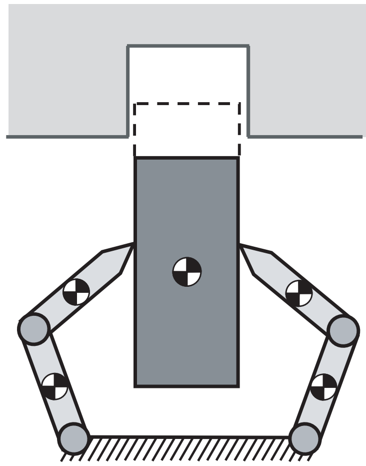

Fig. 3. A peg-in-hole insertion

w_i. By appropriately assigning a set of values to the weights depending on the required task accuracy, we can determine the weighting matrix $\boldsymbol{T}$ which is oriented to the task.

The singular value decomposition of the weighting output controllability matrix $\boldsymbol{N}_T$ can be described as

$$\boldsymbol{N}_T = \sum_{i=1}^{6} \sigma_{Ti} \boldsymbol{u}_{Ti} \boldsymbol{v}_{Ti}^T \tag{18}$$

where $\sigma_{T1} \geq \sigma_{T2} \geq \ldots \geq \sigma_{T6} > 0$ are the singular values, and $\boldsymbol{u}_{Ti}$ is a corresponding singular vector.

A task-oriented measure μ_T is given by inverse of a condition number for the weighting output controllability matrix $\boldsymbol{N}_T$, which is

$$\mu_T = \sigma_{T6}/\sigma_{T1} \leq 1.0 \tag{19}$$

Therefore, the greater the value of the task-oriented measure μ_T gains, the more accurate for the specified task the manipulation system achieves. We show the simulation examples of optimal grasp and task-oriented handling by using the task-oriented measure in the following section.

IV. SIMULATION EXAMPLES

A. Optimal Grasp for Peg-in-hole Insertion

Figure 3 shows that the hand manipulates the rectangular object against a gravity and put it in a hole. For this peg-in-hole insertion task, we obtain the optimal grasp based on the task-oriented measure μ_T of (19).

As shown in Fig. 4, we employ the hand with two two-jointed fingers in a plane such that the hand becomes non-redundant. It is assumed that the rectangular object locates on the y axis of the base frame $\{U\}$ and its orientation is $\phi = 0$ deg, which is gripped by the two fingers with frictional point contacts at the same height y_t and y_c with respect to the base frame $\{U\}$ and the object frame $\{O\}$, respectively. We assume that the hand does not slip on the object at any contact points by exerting the appropriate internal forces.

Each of the links of the finger has unit length, unit mass, and unit moment of inertia. The mass center of each link coincides with its centroid, and the distance between the first joint of the two fingers is unit length. The object has unit mass m_O and unit moment of inertia I_O, respectively.

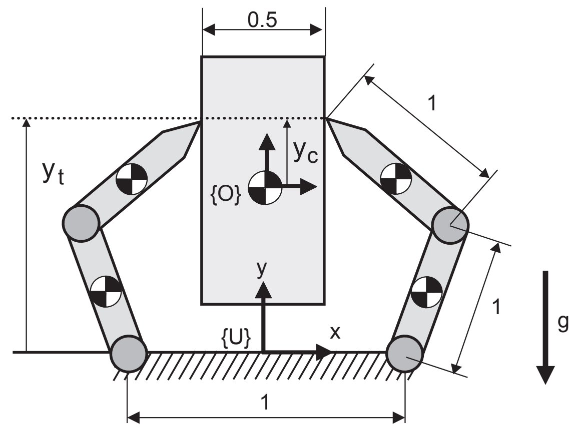

Fig. 4. The two-fingered hand and its physical parameters

In this section, we explore the optimal grasp for a peg-in-hole insertion by changing the height y_t and y_c. The weighting matrix $\boldsymbol{T}$ of (17) for the planar task can be described as

$$\boldsymbol{T} = \mathrm{diag}(w_x,\ w_y,\ w_\phi) \tag{20}$$

where w_x, w_y and w_ϕ are the weights in x, y direction and in direction of rotation ϕ, respectively. In general, the peg-in-hole insertion needs higher task accuracy in the x direction and the direction of rotation ϕ than in the y direction without the object colliding with an environment. In this simulation, the weighting matrix is set as $\boldsymbol{T} = \mathrm{diag}(20,\ 1,\ 20)$.

Fig. 5(a) shows the contour map of the task-oriented measure μ_T for the various values of y_t and y_c. The sign $\bullet$ indicates the optimal values which has the maximum task-oriented measure. The corresponding configuration is described as Fig. 5(b).

From this contour map, the higher the height y_t of the finger tip is, the larger the value of the task-oriented measure is. This means that the more the fingers stretch, the more optimal the grasp can be. However, the value of the task-oriented measure becomes lower drastically around $y_t = 2$, where the fingers get to stretch completely. This means the grasp gets into unstable for the task since the hand becomes the singular configuration.

On the other hand, the longer the length y_c of the contact point position is, the larger the value of the task-oriented measure becomes. This means that the grasp of which contact points locate upper than the object's mass center can come to be more optimal than that of which contact points locate lower than the mass center.

Therefore, to make the peg-in-hole insertion task more accurate, the fingers stretch suitably and grasp the object with the higher contact point position than the object's mass center as shown in Fig. 5(b). These results correspond with our practical experiences for the peg-in-hole insertion.

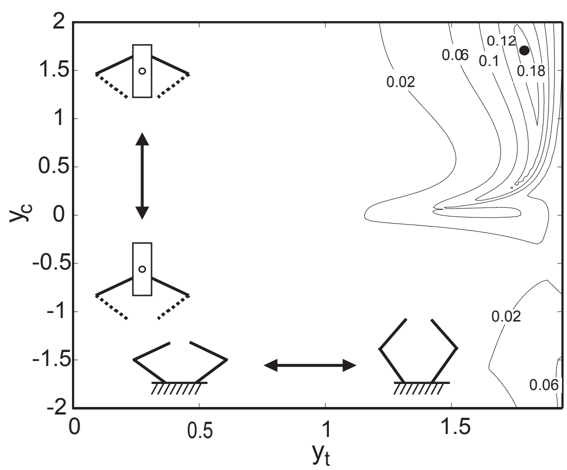

(a) Value of task-oriented measure μ_T

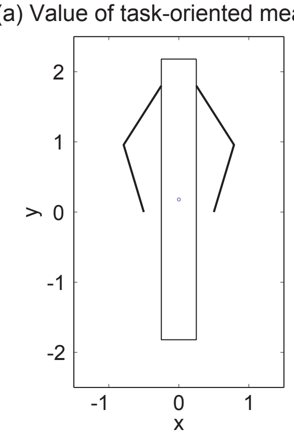

(b) A simulated optimal grasp

Fig. 5. Task-oriented measure for various hand configuration in peg-in-hole insertion task

B. Task-oriented Handling for Baton Twirling

This section takes up a baton twirling problem as a simple manipulation example using the proposed task-oriented measure. As shown in Fig. 6, employing a three two-jointed fingers, the baton is rotated 180 degrees counterclockwise about its mass center. Each finger has the same physical parameters as the model shown in Fig. 4. The initial object position is $(x,\ y) = (0,\ 1.5)$, and the object's mass and moment of inertia are $m_O = 5$ and $I_O = 1$, respectively.

The three-fingered hand regrasps the baton three times to achieve the half revolution of the baton. The switching sequence of the regrasping is shown in Fig. 7. When the baton's orientation is initially $\phi = 0$ deg, the hand grasps the baton at rest. While $0 < \phi < 30$ deg, the fingers 1 and 2 rotate the baton and never change the positions of the contact points. When $\phi = 30$ deg, the finger 3 regrasps the baton and the finger 1 is released simultaneously. After this, the fingers 2 and 3 rotate the baton while $30 < \phi < 80$ deg. As shown in Fig. 7, the hand switches the fingers 1, 2 and 3 one after another when $\phi = 30,\ 80$ and 145 deg.

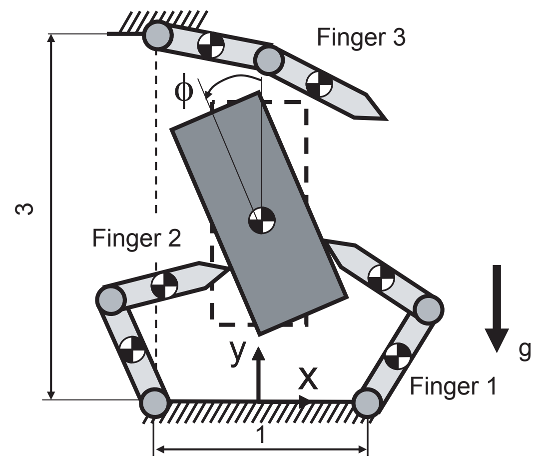

Fig. 6. A baton twirling by the three-fingered hand

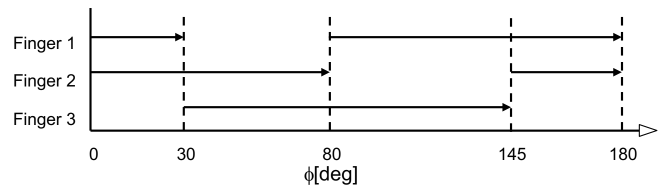

Fig. 7. The switching sequence of regrasping

By using the task-oriented measure μ_T, we obtain not only the optimal initial contact point but the optimal contact point of the regrasping finger based on the switching sequence. It is assumed that the contact points do not change between the regrasping. In this simulation, the following optimization problem is solved to find the optimal contact points.

maximize:	the task-oriented measure μ_T
subject to:	force closure condition and friction constraint
given:	baton's location $\boldsymbol{x}_O$ and weighting matrix $\boldsymbol{T}$
find:	contact point

Each of the sequence requires the different manipulation performance. Thus we change the weighting matrix based on the required performance of each sequence. In this simulation, we set the weighting matrix $\boldsymbol{T}$ as follows:

$$\boldsymbol{T} = \text{diag}(20,\ 20,\ 1) \qquad \text{when } \phi = 0,\ 30,\ \text{and } 80 \text{ deg}$$
$$\boldsymbol{T} = \text{diag}(20,\ 20,\ 20) \qquad \text{when } \phi = 145 \text{ deg}$$

While the baton's orientation is $0 \leq \phi < 145$ deg before the final sequence, the hand rotates the baton by accurately matching the center of rotation with baton's mass center. The hand requires the high accuracy in the x and y directions. Thus we make the weight values in the x and y directions greater than that in the direction of rotation. However, in the final sequence which is $145 \leq \phi \leq 180$ deg, the hand accurately stop the motion of the baton at the moment of achieving $\phi = 180$ deg. Therefore the hand requires the high accuracy in not only the x and y directions but also the direction of rotation. We set the same magnitude in the three directions at the final regrasping.

Figure 8(a) shows the optimal task-oriented baton twirling using the above-mentioned optimization problem. At $\phi = 30$, 80 and 145 deg, the dashed lines indicate the optimal configuration of the regrasping finger obtained from the optimization problem. Figure 8(b) shows the value of the task-oriented measure μ_T. When $\phi = 30$, 80 and 145 deg, its value changes greatly because the finger regrasps the baton. In this simulation, the regrasping gains the greater value of μ_T than that just before the regrasping.

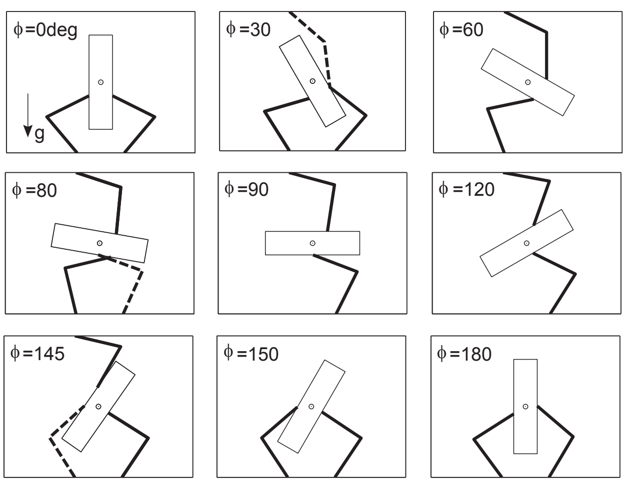

(a) A simulated baton-twirling

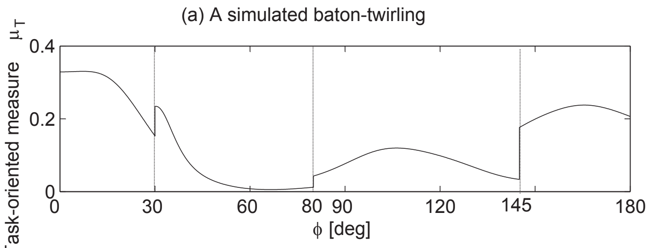

(b) The task-oriented measure

Fig. 8. A simulated baton twirling and its task-oriented measure

V. CONCLUSION

The present paper proposed a novel quality measure for choosing a grasp with high task accuracy to achieve a specified task using the concept of the output controllability. The usefulness of the quality measure are shown by two simulations concerning the optimal grasp for a peg-in-hole insertion task and the task-oriented handling for a baton twirling. We are now planning to conduct experiments by using the NDA Hand in order to show the validity of the proposed task accuracy measure for a real robotic hand.

There are some limitations for applying the proposed quality measure that the robotic hand should be non-redundant such that the matrix $\boldsymbol{M}_{sys}$ in (7) could be invertible. With the advent of humanlike dexterous hand such as DLR Hand [2], the formulation of the quality measure which is applicable to the redundant fingers is one of our future work.

REFERENCES

[1] Ch. Borst, M. Fischer and G. Hirzinger, "A fast and robust grasp planner for arbitrary 3D objects," Proc. IEEE Int. Conf. on Robotics and Automation, pp.1890-1896, 1999.

[2] Ch. Borst, M. Fischer, S. Haidacher, H. Liu and G. Hirzinger, "DLR hand II: experiments and experience with an anthropomorphic hand," Proc. IEEE Int. Conf. on Robotics and Automation, pp.702-707, 2003.

[3] C. Ferrari and J. Canny, "Planning optimal grasps," Proc. IEEE Int. Conf. on Robotics and Automation, pp.2290-2295, 1992.

[4] B. Friedland, "Controllability index based on conditioning number," Trans. of ASME, J. Dynamics Systems, Measuremet and Control, pp.444-445, December 1975.

[5] C. D. Johnson, "Optimization of a certain quality of complete controllability and observability for Linear Dynamical Systems," Trans. of ASME, J. Basic Engineering, pp.228-238, June 1969.

[6] T. Kailath, "Linear systems," Prentice-Hall Inc., 1980.

[7] D. Kirkpatrick, B. Mishra and C.K. Yap, "Quantitative Steinitz's theorems with applications to multifingered grasping," Proc. ACM Symp. on Theory of Computing, pp.341-351, 1990.

[8] E. Kreindler and P. E. Sarachik, "On the concepts of controllability and observability of linear systems," IEEE Trans. on Automatic Control, vol.9, no.2, pp.129-136, 1964.

[9] Z. Li and S.S. Sastry, "Task-oriented optimal grasping by multifingered robot hands," IEEE Journal of Robotics and Automation, vol.4, no.1, pp.32-44, 1988.

[10] Z. Li, P. Hsu and S.S. Sastry, "Grasping and coordinated manipulation by a multifingered robot hand," The Int. J. of Robotics Research, vol.8, no.4, pp.33-50, 1988.

[11] B. C. Moore, "Principal component analysis in linear systems: controllability, observability and model reduction," IEEE Trans. Automatic Control, vol.26, no.1, pp.17-32, 1981.

[12] R.M. Murray, Z. Li and S.S. Sastry, "A Mathematical Introduction to Robotic Manipulation," CRC Press, 1993.

[13] N. Pollard, "Parallel methods for synthesizing whole-hand grasps from generalized prototypes," Technical Report AI-TR 1464, MIT Artificial Intelligence Laboratory, 1994.

[14] G. Strang, "Linear algebra and its application, third edition," Thomson Learing, 1988.

[15] T. Yamawaki and M. Yashima, "Effect of Gravity on Manipulation Performance of Robotic arm," Proc. IEEE Int. Conf. on Robotics and Automation, pp.1120-1125, 2007.

[16] T. Yamawaki and M. Yashima, "Task Accuracy Measure based on Dynamic Process for Cooperating Manipulation System," Proc. IEEE Int. Conf. on Mechatronics and Automation, 2008.

[17] T. Yamawaki, S. Asano, H. Miyashita and M. Yashima, "Robotic catching with precision grasp by vision," Proc. IEEE Int. Conf. on Robotics and Biomimetics, 2008. (to be submitted)